

Fast-Passage Effects in the Nuclear Magnetic Resonance of Fe⁵⁷ in Pure Iron Metal*

DAVID L. COWAN AND L. WILMER ANDERSON

University of Wisconsin, Madison, Wisconsin

(Received 23 March 1964)

The nuclear magnetic resonance of Fe⁵⁷ in pure iron metal has been examined. The results of the experiments have been analyzed in terms of Portis' theories of saturation and fast passage in inhomogeneously broadened spin systems. The principal results are the following: The value of the enhancement factor for iron $\eta=2000$ independent of temperature, the values of the spin-lattice relaxation time $T_1=0.25$ msec at $T=295^\circ\text{K}$, and $T_1=1.3$ msec at $T=77^\circ\text{K}$, and the fact that the dispersion mode of the nuclear susceptibility is coupled out into the power absorbed more strongly than the absorption mode (in the limit of zero saturation). In addition it is found that the distribution of hyperfine fields is plotted directly due to fast-passage effects. This is identified as a fast-passage effect by the observation that the signal amplitude does not increase linearly with the modulation amplitude and by other tests.

INTRODUCTION

THE first observation of nuclear magnetic resonance in a ferromagnet was made by Portis and Gossard¹⁻³ using a sample of metallic Co. They found that the resonant absorption of power was exceedingly intense and that the dispersion mode of the nuclear susceptibility contributed strongly to the power absorption. The intense resonant absorption was shown to result from an interaction of the nuclei and the domain walls in the sample. As the domain walls move in response to the applied rf magnetic field, the nuclei in the domain walls experience a rf magnetic field, which is enhanced in amplitude over the applied field by a large factor ($\sim 10^3$ – 10^4). The observed power absorption has been interpreted as arising from a modulation of the domain wall loss by the nuclear susceptibility induced by the enhanced rf magnetic field. Fe⁴⁻⁶ and Ni^{7,8} have also been examined by nuclear magnetic resonance and show similar effects.

This paper presents the results of an investigation of the nuclear magnetic resonance of unenriched Fe powder. The results are interpreted in terms of theories developed by Portis⁹⁻¹¹ on fast passage and saturation effects in spin systems having spectral distributions. By examining the changes in the nuclear resonance signal

as a function of applied rf magnetic field and modulation frequency, values have been obtained for the enhancement factor, the spin-lattice relaxation time, and the amount of mode mixing. It has also been found possible to plot directly the distribution of hyperfine fields at the Fe⁵⁷ nuclei using phase-sensitive detection.

EXPERIMENTAL TECHNIQUES

The samples used in these experiments have been prepared from carbonyl iron. The carbonyl iron originally contained about 0.1 or 0.2% of nonmetallic impurity, mostly oxygen and a small amount of carbon and nitrogen. Of several metallic impurities the nickel content was highest being about 40 ppm. Solid iron samples of bulk density (~ 7.86 g/cc) were prepared from the carbonyl iron by pressing and sintering (at 1200°C) under a very dry hydrogen atmosphere. This procedure removes the nonmetallic impurities. The iron slug was then filed and those filings, which passed through a 325-mesh sieve were retained. These were then annealed under a hydrogen atmosphere at about 700°C to remove the strain produced by filing.^{12,13}

The oscillator used in these experiments is a modified version of one described by Knight.¹⁴ This circuit is sensitive only to power absorbed and is designed to operate at high rf levels. The oscillator is frequency modulated. The output of the oscillator is amplified by conventional amplifiers and recorded with the help of a phase-sensitive detector locked to the fundamental modulation frequency.

EXPERIMENTAL OBSERVATIONS AND ANALYSIS

A. Room-Temperature Results

It has been shown by spin-echo experiments that for natural unenriched Fe the magnetic resonance of Fe⁵⁷

* This research has been supported in part by the National Science Foundation and in part by University Research Funds provided by the Wisconsin Alumni Research Foundation.

¹ A. C. Gossard and A. M. Portis, Phys. Rev. Letters **3**, 164 (1959).

² A. M. Portis and A. C. Gossard, J. Appl. Phys. Suppl. **31**, 205S (1960).

³ A. C. Gossard, Ph. D. thesis, University of California, 1960 (unpublished).

⁴ A. C. Gossard, A. M. Portis, and W. J. Sandle, Phys. Chem. Solids **17**, 341 (1961).

⁵ C. Robert and J. M. Winter, Compt. Rend. **250**, 3831 (1960).

⁶ J. I. Budnick, L. J. Bruner, R. J. Blume, and E. L. Boyd, J. Appl. Phys. **32**, 120S (1961).

⁷ L. H. Bruner, J. I. Budnick, and R. J. Blume, Phys. Rev. **121**, 83 (1961).

⁸ R. L. Streever and L. H. Bennett, Phys. Rev. **131**, 2000 (1963).

⁹ A. M. Portis, Phys. Rev. **91**, 1071 (1953).

¹⁰ A. M. Portis, Phys. Rev. **100**, 1219 (1955).

¹¹ A. M. Portis, Sarah Mellon Scaife Radiation Laboratory, University of Pittsburgh, Technical Note No. 1, November 1955 (unpublished). See also, M. Weger, Bell System. Tech. J. **39**, 1013 (1960); G. Feher, Phys. Rev. **114**, 1219 (1959).

¹² This treatment is not expected to leave any appreciable amount of H₂ in the lattice. See D. P. Smith, *Hydrogen in Metals* (University of Chicago Press, Chicago, 1948); H. B. Wahlen (private communication). Nevertheless, this was checked by a final anneal in ultrahigh vacuum. None of the observed properties were changed.

¹³ A few experiments were performed with the 10- μ spherical particles of carbonyl iron powder as received. The linewidth was

is characterized by equal longitudinal and transverse relaxation times (i.e., $T_1 = T_2$) and an inhomogeneously broadened line.^{15,16} Portis¹¹ has shown that under these conditions it is appropriate to view the resonance line as composed of a series of noninteracting homogeneous spin packets with a distribution given by the distribution of local magnetic fields at the nuclei. Under conditions of saturation the time required to cross one of these packets will be $\sim H_1/\omega_m H_m$, where $2H_1$ is the peak transverse rf field, ω_m the modulation frequency, and γH_m the modulation amplitude. If this time is short compared to the spin-lattice relaxation time and if the adiabatic condition is satisfied (i.e., $\gamma H_1^2 > \omega_m H_m$), each packet will be traversed under conditions of adiabatic fast passage. This leads to a susceptibility with a peak amplitude nearly independent of modulation amplitude, and a line shape directly reflecting the distribution of local magnetic fields. As $\epsilon = H_m \omega_m T_1 / H_1$ approaches zero, the usual slow passage susceptibility is obtained. In the intermediate case where $\epsilon < 1$, Portis^{10,11} finds for that part of the susceptibility periodic at ω_m

$$\chi'(\omega) = \frac{\pi}{2} \chi_0 \omega \frac{\partial}{\partial \omega_0} \left\{ \frac{2}{\pi} \int_0^\infty \frac{\omega' h(\omega', \omega_0) d\omega'}{\omega'^2 - \omega^2} \right\} \gamma H_m \cos \omega_m t$$

$$+ \frac{1}{4} \pi \chi_0 \omega \epsilon [1 + (\omega_m T_1)^2]^{-1/2} h(\omega, \omega_0)$$

$$\times \sin(\omega_m t - \tan^{-1} \omega_m T_1) + O(\epsilon^3), \quad (1)$$

where $h(\omega, \omega_0)$ is the normalized distribution of local fields. The first term is the slow-passage dispersion derivative in phase with the modulation. The second term is the fast-passage contribution proportional to $h(\omega, \omega_0)$ and shifted in phase from the modulation.

Figure 1 shows the signals observed in natural Fe at room temperature with the phase-sensitive detection in phase and in quadrature with the applied modulation. The signal in quadrature represents a distribution of local fields, $h(\omega, \omega_0)$, which is nearly Lorentzian (there is a small asymmetrical broadening on the low-frequency side of the line) with a half-width at half-power of $\Delta\omega/2\pi = 8 \times 10^3$ cps. The in-phase signal is the type of dispersion-derivative slow-passage signal expected with this $h(\omega, \omega_0)$.

If we ignore the low-frequency asymmetry in $h(\omega, \omega_0)$ and substitute $h(\omega, \omega_0) = (1/\pi \Delta\omega) \{1/[1 + (\omega - \omega_0/\Delta\omega)^2]\}$ in Eq. (1), we find for the ratio of "fast passage" to "slow passage" susceptibility at $\omega = \omega_0$.

$$\chi_{\text{fast}}/\chi_{\text{slow}} = \Delta\omega \omega_m T_1 / \gamma \eta H_x [1 + (\omega_m T_1)^2]^{1/2}, \quad (2)$$

about 40% greater than in the heat-treated samples, and the fast-passage results were similar to those in the heat-treated samples.

¹⁴ W. D. Knight, Rev. Sci. Instr. **32**, 95 (1961).
¹⁵ M. Weger, E. L. Hahn, and A. M. Portis, J. Appl. Phys. **32**, 124S (1961).

¹⁶ C. Robert and J. M. Winter, Arch. Sci. (Geneva) **13**, 433 (1960).

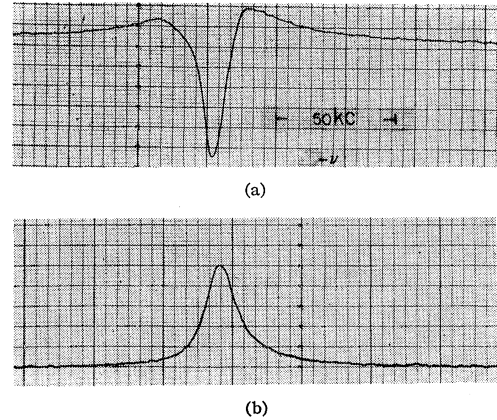


FIG. 1. Resonance signals observed with phase-sensitive detection. $H_x = 15$ mG, $\omega_m/2\pi = 320$ cps. (a) Detection in phase with the modulation. This trace is mostly the derivative of the dispersion mode of the nuclear susceptibility. (b) Detection at 90° to the modulation. This trace represents the distribution of local magnetic fields at the nuclei of the sample.

where the domain-wall enhancement is included by writing $H_1 = \eta H_x / 2$.¹⁷

Figure 2 shows a systematic study of the adiabatic fast-passage effects in the NMR of Fe⁵⁷ at room temperature as a function of modulation frequency. These were all run with an rf voltage of about 0.35 V rms across the coil, from which we calculate $H_x \sim 15 \times 10^{-3}$ G. For $\omega_m/2\pi = 40$ cps, the signal is almost pure slow passage, but for $\omega_m/2\pi = 160$ cps, fast-passage effects are making an appreciable contribution. When $\omega_m/2\pi = 320$ cps, the relative amount of fast passage has continued to increase, and the phase of the fast-passage component has begun to move away from 90° and distort the signal at 0° phase. With $\omega_m/2\pi = 1050$ cps, the fast-passage signal is shifted in phase from 90° toward 180° . The in-phase component of the fast-passage signal is larger than the slow-passage signal, and the 0° resonance turns over. Since the dispersion derivative is narrower than the field distribution, we see the slow-passage signal pushing back up at the center of the fast passage line at 0° .

The results shown in Fig. 2 can be compared with calculations based on Eq. (1), and values can be found for the two unknown quantities η and T_1 . Since most of the dependence is in the form T_1/η , we can solve for this ratio easily. We find $T_1/\eta = 125 \times 10^{-9}$ sec. When the modulation frequency becomes high enough for $\omega_m T_1$ to be of the order of 1, then T_1 enters Eq. (1) independently of the ratio T_1/η , and from the observed signal we can estimate with somewhat less accuracy $T_1 \sim 200 \times 10^{-6}$ sec. This implies $\eta = 1600$. These values for T_1 and η fit all the data in Fig. 2 quite well.

Our confidence in this interpretation is strengthened by the verification of Eq. (2) as a function of H_x over a wide range of applied rf fields. In addition at $\omega_m/2\pi$

¹⁷ The expression $\chi'_{\text{fast}}/\chi'_{\text{slow}}$ is evaluated at $\omega = \omega_0$ and the amplitude of both χ'_{fast} and χ'_{slow} is measured from the baseline.

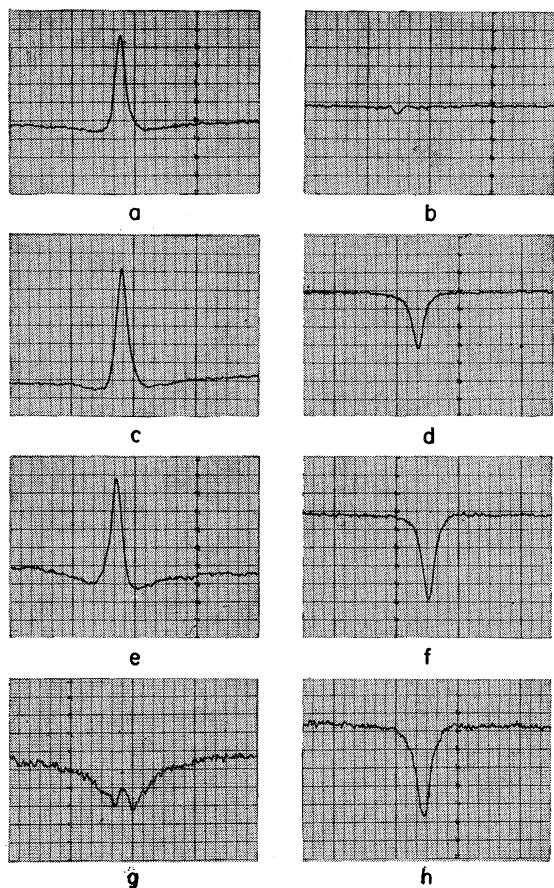


FIG. 2. Resonance signals as a function of modulation frequency ω_m increasing from top to bottom. Signals on the left are at 0° phase, signals on the right at 90° phase. $H_x = 15$ mG. (a) $\omega_m/2\pi = 40$ cps 0° phase; (b) $\omega_m/2\pi = 40$ cps 90° phase; same gain as (a); (c) $\omega_m/2\pi = 160$ cps 0° phase; (d) $\omega_m/2\pi = 160$ cps 90° phase, same gain as (c); (e) $\omega_m/2\pi = 320$ cps 0° phase; (f) $\omega_m/2\pi = 320$ cps 90° phase, same gain as (e); (g) $\omega_m/2\pi = 1050$ cps 0° phase; (h) $\omega_m/2\pi = 1050$ cps 90° phase, same gain as (g).

$= 320$ cps and $H_x = 15$ mG, ϵ was varied from 0.6 to 1.8 by increasing the modulation amplitude. It was found that the amplitude of the fast-passage signal grows more slowly than the modulation amplitude, increasing a factor of 1.7 over-all (the slow-passage signal was observed to be directly proportional to H_m in all cases).¹¹ When the rf level is increased to $H_x = 45$ mG so that ϵ ranges from 0.2 to 0.6, the fast-passage signal amplitude is directly proportional to modulation amplitude. This is a unique characteristic of fast-passage effects in an inhomogeneously broadened line for which $T_2 \sim T_1$. Portis looked for and did not observe these effects in Co. He attributed this to spin-spin interactions ($T_2 < T_1$ in Co).^{1,2}

Finally we should point out that these values of η and T_1 are consistent with the conditions which must be satisfied in order that Eq. (1) be valid. The line is inhomogeneously broadened, the resonance is saturated, $\epsilon < 1$, and the adiabatic condition is satisfied.¹¹

The value for the enhancement factor can be checked

by studying the slow-passage signal as a function of applied rf field. Portis has shown that the dispersion part of the susceptibility may be obtained by integrating over the Bloch solutions for the individual spin packets, weighted by the inhomogeneous broadening envelope.¹¹ This gives

$$\chi'(\omega) = \frac{1}{2} \chi_0 \omega T_1 \int_0^\infty \frac{(\omega - \omega') T_1 h(\omega', \omega_0) d\omega'}{1 + [\gamma(\eta H_x/2) T_1]^2 + (\omega - \omega')^2 T_1^2}.$$

At high rf levels the 1 in the denominator can be neglected. Inserting the observed Lorentzian line shape $h(\omega, \omega_0)$ and integrating gives

$$\chi'(\omega) = \frac{1}{2} \chi_0 \omega_0 \frac{\omega_0 - \omega}{[\gamma(\eta H_x/2) + \Delta\omega]^2 + (\omega_0 - \omega)^2}.$$

Portis and Gossard used the amplitude dependence of this expression to find the enhancement factor for Co.² In our case the recorder plots the derivative of the susceptibility ($\times H_1$) and we expect to find a full-width at half-height $\delta\omega = 2(\sqrt{5} - 2)^{1/2}(\gamma H_1 + \Delta\omega)$ and a signal amplitude $(\partial\chi'/\partial\omega)_{\omega=\omega_0} \propto 1/(\gamma H_1 + \Delta\omega)^2$. A linear increase in the width of the slow-passage signal is observed as H_x increases from 15 to 90 mG. From this broadening we calculate $\eta = 2000$ for the enhancement factor, in good agreement with our previous result. Figure 3 shows the measured slow-passage amplitudes at $H_x = 15, 45,$ and 90 mG. These results were corrected for oscillator characteristics. The curve represents the expected signal amplitude for $\eta = 2000$. Again the agreement is satisfactory. Using the value $\eta = 2000$ and the previous value for T_1/η , we find $T_1 = 250 \times 10^{-6}$ sec. We believe these values for T_1 and η are somewhat preferable to those obtained from the fast-passage data alone.

Figure 3, also, serves to illustrate what is believed to be the most serious difficulty in applying the results of Eq. (1) to the data. This is that the slow-passage signal is attenuated about 35% at $H_x = 15$ mG. We did not

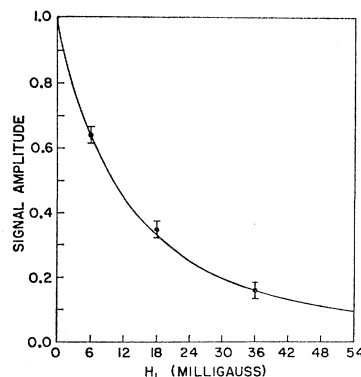


FIG. 3. Amplitude of the derivative of the nuclear dispersion (arbitrary units) as a function of applied rf field amplitude $H_1 = H_x/2$ (Note: this is not the same as $H_1 = \eta H_x/2$ used in the text.) These amplitudes have been corrected for oscillator characteristics, and the error bars indicate reproducibility of the data. The solid line is the expected variation for $\eta = 2000$. (Note: all values of H_1 given on the abscissa of the graph should be increased by a factor 1.25.)

work at a lower rf level because the saturation condition is not well satisfied if H_x is much less than 15 mG. The problem basically is that there are not enough homogeneous spin packets under the inhomogeneously broadened envelope. Since the effects of high rf level also decrease the amplitude of the fast-passage signal, we feel the error introduced by using Eq. (1) and neglecting rf broadening effects is fairly small.

All the above analysis applies only to the dispersion mode of the nuclear susceptibility. Since our oscillator is sensitive only to absorbed power, these effects have been observed as a consequence of the mode mixing in the sample. The question naturally arises as to whether effects of the absorptive part of the nuclear susceptibility can be observed. Portis' analysis of the slow-passage absorption signal for an inhomogeneously broadened line with a Lorentzian distribution of local fields gives¹¹

$$\chi''(\omega) = \frac{1}{2} \chi_0 \omega_0 \frac{\Delta\omega}{(\Delta\omega)^2 + (\omega - \omega_0)^2} (1 + \gamma^2 H_1^2 T_1^2)^{-1/2}.$$

Consequently, $\chi''(\omega)$ saturates at large H_1 relative to $\chi'(\omega)$. This explains why no absorption derivative component is observed in our slow-passage traces. As the rf level is lowered to a value near saturation, some absorption component is observed in the power absorption. In a manner similar to that used by Streever and Bennet,⁸ who studied mode mixing in the NMR of Ni⁶¹, the total power absorption is written $dW/dt \propto \chi''(\omega) + \beta_0 \chi'(\omega)$, where $\chi''(\omega)$ and $\chi'(\omega)$ are the usual slow-passage absorption and dispersion susceptibilities, respectively. From the observed line shapes as a function of H_1 and the known saturation behavior of $\chi''(\omega)$ and $\chi'(\omega)$, we can evaluate β_0 .

Figure 4 shows the observed slow-passage signal when $\gamma H_1 T_1 \sim 1$. This can be compared to Fig. 2(a) where $\gamma H_1 T_1 \sim 3$. The signal has been appreciably distorted by a contribution from the absorption derivative. We estimate from Fig. 4 that $\beta_0 \sim 3$.

This value for β_0 can be checked in a rather rough

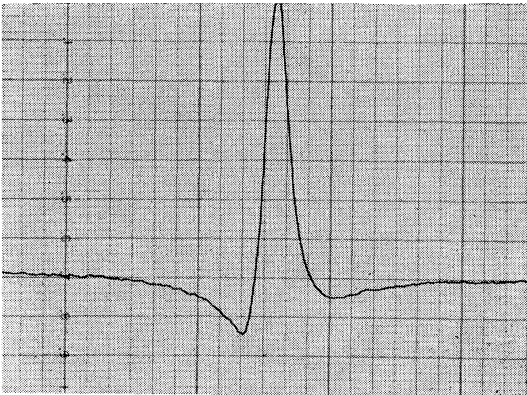


FIG. 4. Distortion of the usual dispersion derivative by a mixing of some nuclear absorption derivative. $\omega_m/2\pi = 40$ cps. $H_x \sim 5$ mG, phase set carefully to 0° to avoid mixing with the residual fast-passage signal.

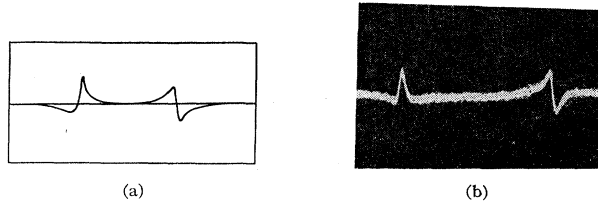


FIG. 5. Oscilloscope trace of the output of the oscillator when the entire line is crossed almost suddenly. The right-hand figure shows the observed signals. $H_x \sim 5$ mG, $\gamma H_m/2\pi \approx 320$ kc/sec, $\omega_m/2\pi = 200$ cps. From left to right the oscillator is swept from below the resonance to above it, and back again. The loss of nuclear magnetization is estimated to be a few percent per passage. The left-hand figure shows the expected shapes (not scaled vertically or horizontally) if $\beta_0 = 3$, the line is Lorentzian, and the experimental conditions are as given above.

fashion by a study of the resonance line under conditions of nonadiabatic passage. The oscillator is frequency modulated with an amplitude much greater than the linewidth, and the output amplified with broad-band amplifiers and displayed directly on an oscilloscope. When the nonadiabatic condition ($\omega_m H_m \gg \gamma H_1^2$) is satisfied, the z component of nuclear magnetization will be practically unaffected by the rf field and the susceptibility will not saturate regardless of the magnitude of $\gamma H_1 T_1$. Jacobsohn and Wangsness¹⁸ have calculated the dispersion and absorption line shapes expected when a Lorentzian line is traversed under these conditions. These signals possess no center of symmetry even though the distribution of local fields is symmetric about ω_0 . The sign of the dispersion signal depends on the direction of sweep while that of the absorption does not.¹⁹ As a result, mixing these signals together can produce a response when $d\omega/dt > 0$ which looks very different from that obtained when $d\omega/dt < 0$. Figure 5 shows the observed signals as the frequency sweeps through the resonance line with $d\omega/dt > 0$ and $d\omega/dt < 0$ (the wiggles characteristic of nonadiabatic passage are damped by the inhomogeneous nature of the line). The fundamental of the incidental amplitude modulation due to the large frequency modulation has been bucked out. The left-hand figure indicates the expected shapes for a Lorentzian line on the assumption $\beta_0 \sim 3$. Since our observed $h(\omega, \omega_0)$ is not exactly Lorentzian and since the signal-to-noise ratio is poor, we believe the agreement is satisfactory.

B. Results Obtained at 77°K

These experiments have been repeated at 77°K using the same sample. The distribution of local fields remains nearly Lorentzian. However, the low-frequency asymmetry observed at room temperature has vanished. The half-width of the distribution of fields is $\Delta\omega/2\pi = 11 \times 10^3$

¹⁸ B. A. Jacobsohn and R. K. Wangsness, Phys. Rev. **73**, 942 (1948). See also, M. Weger, Bell System Tech. J. **39**, 1013 (1960).

¹⁹ The nuclear susceptibility satisfies the relations

$$\begin{aligned} \chi'(\omega + \omega_0) \Big|_{d\omega/dt > 0} &= -\chi'(\omega_0 - \omega) \Big|_{d\omega/dt < 0}, \\ \chi''(\omega + \omega_0) \Big|_{d\omega/dt > 0} &= \chi''(\omega_0 - \omega) \Big|_{d\omega/dt < 0}, \end{aligned}$$

for nonadiabatic passage if $h(\omega, \omega_0)$ is Lorentzian.

cps with a maximum at $\omega_0/2\pi = 46.542$ Mc/sec. Measurements of the width and amplitude of the slow-passage signal versus rf level lead to an enhancement factor essentially unchanged from the room-temperature value, $\eta = 2000$. Traces at 0 and 90° phase setting at modulation frequencies from 20 to 160 cps are consistent with $\eta = 2000$ and $T_1 = 1.3$ msec.

Because of the large amount of fast-passage signal present even at the lowest modulation frequency, we cannot reliably estimate β_0 from the shape of the slow-passage signal plotted out by the recorder. However, observations of the nonadiabatic passage signals on the oscilloscope indicate that $\beta_0 \sim 3$ at $T = 77^\circ\text{K}$, unchanged from the room-temperature value.

DISCUSSION

The value for the enhancement factor found from these experiments, $\eta = 2000$, is in fairly good agreement with the value $\eta = 1500$ given by Robert and Winter,¹⁶ who inferred the enhancement by spin-echo techniques. The theory of domain wall enhancement developed by Portis² and Gossard, leads to values for η of approximately this magnitude.

The situation is more complicated for the relaxation times. The spin echo experiments of Robert and Winter¹⁶ give a relaxation time in reasonable agreement with our result at 77°K, but they found a very weak temperature dependence between 77°K, and room temperature. Spin-echo experiments by Weger, Hahn, and Portis¹⁵ show a nonexponential relaxation behavior, and a relaxation time which increases with increasing rf power. At 77°K they give $T_1 = 0.7$ –11.2 msec and at 295°K, $T_1 = 0.9$ –6.5 msec. They correlate this range of values for T_1 with a distribution of nuclei throughout the sample (i.e., nuclei in the domains, domain walls, and boundaries) and hence indirectly correlate the distribution in T_1 to a distribution of values of η . The shortest times are assumed to correspond to those nuclei in the domain wall since these nuclei have the largest enhancement factor. Presumably, the shortest times T_1 should be compared with our results. Both the experiments of Robert and Winter and Weger, Hahn, and Portis give a substantially longer T_1 at room temperature than our work. Since $T_1 = T_2$ spin-spin interactions are negligible and driven relaxation (as observed in our experiments) is probably the same as free relaxation (as observed in spin-echo experiments). Winter²⁰ has calculated the relaxation time which arises from thermal fluctuations of the domain walls and finds order-of-magnitude agreement with the observed relaxation times. This calculation depends on domain-wall parameters, which are poorly known and may have intrinsic temperature dependence.

Gossard^{3,4} has developed a theoretical expression for

²⁰ J. M. Winter, Phys. Rev. **124**, 452 (1961). See also, M. Weger, Phys. Rev. **128**, 1505 (1962); E. Simanek and Z. Sroubek, Czech. J. Phys. **B11**, 764 (1961).

mode mixing due to modulation of the intrinsic domain-wall loss by the nuclear magnetization. Starting from the Landau-Lifshitz equation of motion for the magnetization

$$\frac{d\mathbf{M}}{dt} = \gamma_e(\mathbf{M} \times \mathbf{H}) - \frac{\lambda}{M^2} \mathbf{M} \times (\mathbf{M} \times \mathbf{H}),$$

he finds $\beta_0 = \lambda/\gamma_e |M|$ where \mathbf{M} is the saturation magnetization, γ_e is the electron gyromagnetic ratio, and λ is a phenomenological damping constant. For Fe, λ is poorly known and structure sensitive but a reasonable value is²⁰ $\lambda \sim 10^9$ sec⁻¹. This is a hundred times too small to explain our observed β_0 . In any event, this theory can hardly account for values of $\beta_0 > 1$ since the damping torque in the Landau-Lifshitz expression becomes larger than the applied torque and the expression is no longer appropriate in that case.

The source of inhomogeneous broadening has been considered by Suhl²¹ and by Friedel and de Gennes.²² Friedel and de Gennes have discussed the contribution to the inhomogeneous broadening in multidomain conducting particles due to the demagnetizing fields near the surface of the sample. They conclude in a material with a low anisotropy, such as iron, the inhomogeneous broadening from this mechanism will be of the order of magnitude of the anisotropy field. In Fe, $\gamma H_A/2\pi \approx 70 \times 10^8$ cps, which is not inconsistent with the observed width. In addition, the increase in width on cooling the sample to 77°K from room temperature is approximately the same as the known increase in H_A . A broadening mechanism introduced by Suhl, which arises because of a nonuniform spin-wave density throughout the Bloch wall can give a maximum contribution of about 15×10^8 cps at room temperature. The broadening due to this mechanism will be very small at 77°K. No narrowing of the distribution of this type is observed.

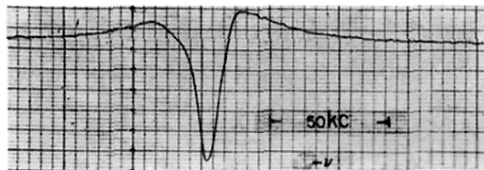
Finally, we wish to point out that the distribution of local fields is usually the item of interest and there can be appreciable advantages to plotting $h(\omega, \omega_0)$ directly with phase-sensitive detection. This may, for instance, simplify the interpretation of overlapping lines in dilute Fe alloys. In addition long term stability and drift characteristics of a spectrometer are greatly improved with detection at 90° to the modulation.

Notes added in proof. Professor A. M. Portis has informed us that he has improved the previous treatment of the relation between the absorption and dispersion signal intensities.

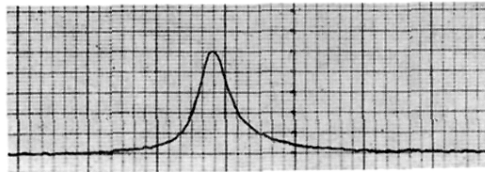
Since this article was submitted we have made a direct determination of the enhancement factor in Fe by the technique of rotary saturation and find $\eta \sim 2000$ in agreement with the value given in this paper.

²¹ H. Suhl, Bull. Am. Phys. Soc. **5**, 175 (1960).

²² J. Friedel and P. G. de Gennes, Compt. Rend. **251**, 1283 (1961).



(a)



(b)

FIG. 1. Resonance signals observed with phase-sensitive detection. $H_z = 15$ mG, $\omega_m/2\pi = 320$ cps. (a) Detection in phase with the modulation. This trace is mostly the derivative of the dispersion mode of the nuclear susceptibility. (b) Detection at 90° to the modulation. This trace represents the distribution of local magnetic fields at the nuclei of the sample.

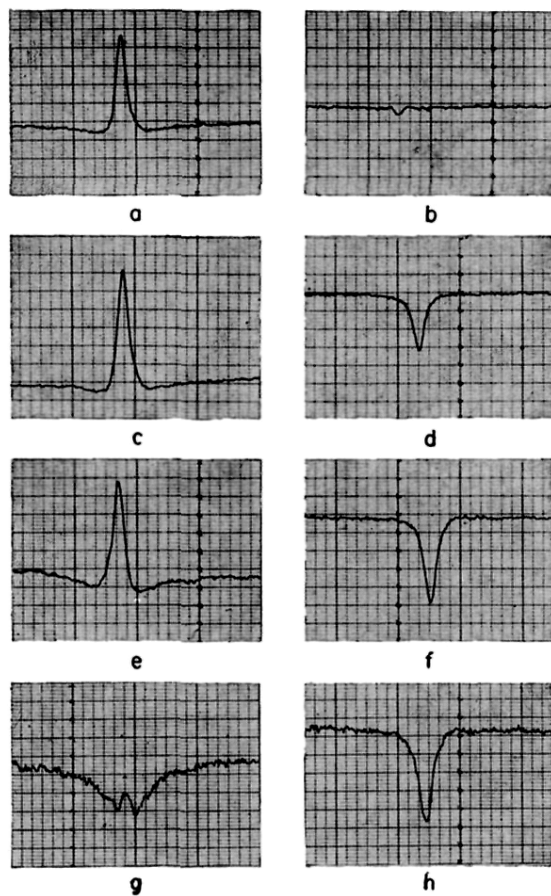


FIG. 2. Resonance signals as a function of modulation frequency ω_m increasing from top to bottom. Signals on the left are at 0° phase, signals on the right at 90° phase. $H_x = 15$ mG. (a) $\omega_m/2\pi = 40$ cps 0° phase; (b) $\omega_m/2\pi = 40$ cps 90° phase; same gain as (a); (c) $\omega_m/2\pi = 160$ cps 0° phase; (d) $\omega_m/2\pi = 160$ cps 90° phase, same gain as (c); (e) $\omega_m/2\pi = 320$ cps 0° phase; (f) $\omega_m/2\pi = 320$ cps 90° phase, same gain as (e); (g) $\omega_m/2\pi = 1050$ cps 0° phase; (h) $\omega_m/2\pi = 1050$ cps 90° phase, same gain as (g).

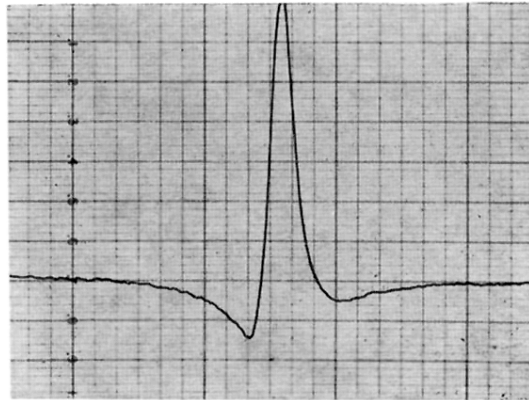


FIG. 4. Distortion of the usual dispersion derivative by a mixing of some nuclear absorption derivative. $\omega_m/2\pi=40$ cps. $H_x\sim 5$ mG, phase set carefully to 0° to avoid mixing with the residual fast-passage signal.

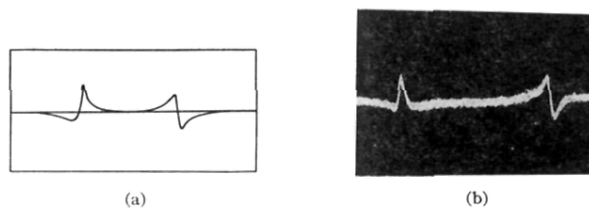


FIG. 5. Oscilloscope trace of the output of the oscillator when the entire line is crossed almost suddenly. The right-hand figure shows the observed signals. $H_z \sim 5$ mG, $\gamma H_m / 2\pi \approx 320$ kc/sec, $\omega_m / 2\pi = 200$ cps. From left to right the oscillator is swept from below the resonance to above it, and back again. The loss of nuclear magnetization is estimated to be a few percent per passage. The left-hand figure shows the expected shapes (not scaled vertically or horizontally) if $\beta_0 = 3$, the line is Lorentzian, and the experimental conditions are as given above.